Tunable subpicosecond dye laser amplified at 1 kHz by a cavity-dumped, *Q*-switched, and mode-locked Nd:YAG laser

Vincent J. Newell, F. W. Deeg, S. R. Greenfield, and M. D. Fayer

Department of Chemistry, Stanford University, Stanford, California 94305

Received September 19, 1988; accepted November 8, 1988

Tunable subpicosecond pulses are generated by synchronously pumping a dye laser with the pulse-compressed and frequency-doubled output of an acousto-optically mode-locked cw Nd:YAG laser. The pulses are amplified at a repetition rate of 1 kHz, using the frequency-doubled output of a cavity-dumped, acousto-optically mode-locked, *Q*-switched, cw pumped Nd:YAG laser. Amplified transform-limited pulses of 150–300 fsec have been obtained in the wavelength range of 560–680 nm (R6G and DCM dyes) with a maximum energy of 50 μJ. Since there is no intracavity prism compensation and no recompression stage after the amplifier, the system is tuned easily with a single-plate birefringent filter; only cavity-length adjustment is required. An electronic control system eliminates amplitude fluctuations caused by timing jitter between the 70-psec amplifying pulses and the dye pulses.

1. INTRODUCTION

In this paper we describe the characteristics of an amplified subpicosecond dye laser system that is readily tunable over broad spectral regions. The principal features of this system are the ease with which it can be tuned, high peak powers, transform-limited pulses with durations of <300 fsec, and a 1-kHz repetition rate. The output of a cw mode-locked Nd:YAG laser is pulse compressed and frequency doubled. The frequency-doubled pulse stream is used to pump a dye laser synchronously. Ultrashort-pulse synchronous pumping of mode-locked dye lasers has proved to be a reliable method for the generation of tunable femtosecond pulses.[1,2] This method provides tunable pulses over a wide wavelength range by avoiding intracavity saturable absorbers that restrict the tunability in hybrid mode-locked[3] and colliding-pulse mode-locked[4] laser systems.

Amplification of the optical pulses is achieved by pumping a three-stage amplifier chain with frequency-doubled pulses from a cavity-dumped, *Q*-switched, and mode-locked Nd:YAG laser operating at a repetition rate of 1 kHz (Fig. 1). The cavity-dumped Nd:YAG laser produces 1-mJ IR pulses that, when frequency doubled, generate 700-μJ pulses of 532-nm light to pump the three stages of the amplifier. The output of this laser is similar to that produced from a regenerative amplifier, but this is a self-contained laser, which has a number of advantages. The cw mode-locked laser and the *Q*-switched and mode-locked amplifying laser use the same master rf oscillator[5] as the frequency source for their respective mode lockers. This ensures that the pulse-to-pulse separations are identical in the two lasers. The timing of the amplifier can then be set by phase shifting the rf signal into the amplifying laser's mode locker. Amplitude fluctuations that are due to timing jitter between the dye pulses and the amplifying pulses are eliminated by a straightforward feedback circuit that controls the phase of the rf going into the amplifying laser's mode locker. In addition to removing the effects of timing jitter and any long-time-scale phase drift, the feedback system stabilizes the intensity of the amplified pulses by modulating the amplifier gain to correct for frequency intensity variations of 100 Hz and lower. In a standard regenerative amplifier, an optical pulse from the cw laser is injected into the regenerative cavity, and electronic phase shifting is not possible.

2. THE *Q*-SWITCHED, MODE-LOCKED, AND CAVITY-DUMPED Nd:YAG LASER

To boost the dye laser pulse energies into the range of tens of microjoules, optical amplification is necessary. We use a frequency-doubled, cavity-dumped, *Q*-switched, and mode-locked Nd:YAG laser to pump a dye amplifier chain. Successful operation of a cavity-dumped, mode-locked, and *Q*-switched laser was demonstrated recently.[6] This type of laser provides an excellent high-repetition-rate source for amplification of picosecond and subpicosecond dye laser pulses. The pulse energies are large enough for net amplifier gains of several tens of thousands to be obtained.

The laser uses a thin-film dielectric polarizer (Burleigh Model 19R) and an electro-optic Pockels cell, which uses a lithium niobate ($LiNbO_3$) crystal (Inrad) to cavity dump the pulse. Because of the high peak intensity in the closed cavity, optical damage to the coated elements can be a major problem. To avoid this problem, the cavity is designed to produce a large laser mode volume, and therefore a reduced peak intensity, in these elements. The cavity is formed with a 2-m-radius-of-curvature convex mirror and a flat mirror. The laser is mode locked at 41 MHz; hence the optical length of the cavity is 183 cm. Although this cavity does give the desired large mode volume in the cavity-dumping elements, it does not do an optimal job of filling the Nd:YAG rod.

The cavity is configured in the following manner. Immediately next to the flat mirror is the acousto-optic mode locker. The mode locker uses a Brewster–Brewster substrate with a 16 mm × 4 mm $LiNbO_3$ transducer that is bonded to the substrate with a cyanoacrylate-based glue. One-half watt of rf power is applied. No cooling of the mode locker is required. This simple process produces a thin, hard bond. After the mode locker is an adjustable iris on an x–z positioner to ensure TEM_{00} operation. Immediately

0740-3224/89/020257-07$02.00

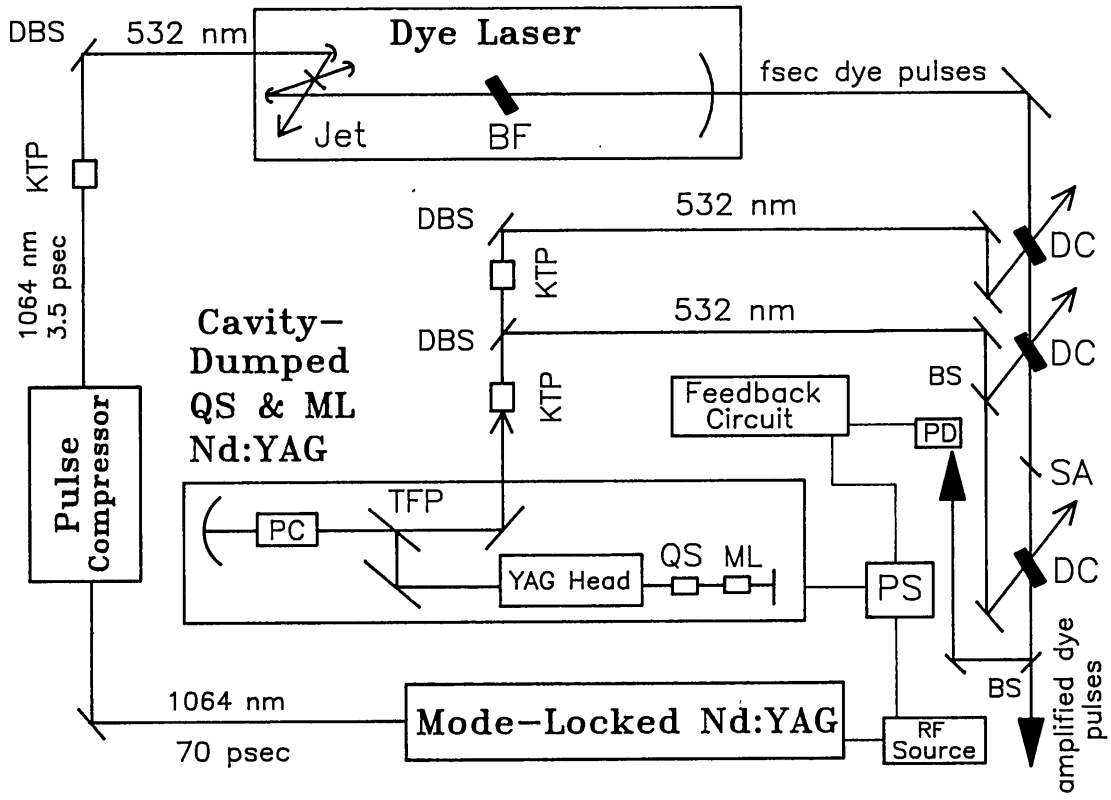

Fig. 1. Amplified subpicosecond dye laser system. BF, Birefringent filter; BS's, beam splitters; DBS, dichroic beam splitter, DC's, dye cells; KTP's, potassium trihydrogen phosphate (frequency-doubling crystals); ML, mode locker; PC, Pockels cell; PD, photodiode; PS, phase shifter; SA, saturable absorber; TFP, thin-film polarizer, QS, *Q* switch.

after the iris is a *Q* switch, which also uses a Brewster–Brewster substrate. The use of Brewster substrates eliminates the need for antireflection coatings on these elements. The *Q* switch requires between 10 and 15 W of power. The transducer is also 16 mm × 4 mm and is water cooled. Because the cyanoacrylate-based glue is water soluble, the *Q*-switch transducer is epoxy bonded to the substrate. The center of the Nd:YAG rod is placed 40 cm away from the optical flat. The rod is 4 mm × 79 mm and is pumped by a single arc lamp with 3.5 to 4.0 kW of dc input. The rod acts as a lens with an effective focal length of 35–40 cm, depending on the amount of current supplied to the lamp.

After the laser head, as close to the curved mirror as mechanical mounting will permit, are the optical elements in the cavity dumper. First there is a 1.06-μm-high reflector at Brewster's angle. This reflects the laser pulse into the Brewster-angle thin-film dielectric polarizer. The net result of these two elements is a small jog in the optical path. The beam after the polarizer is translated but parallel to the beam in the rest of the cavity. The beam then passes through the Pockels cell and hits the curved mirror. The mirror mount holding the curved mirror is on a precision translation stage that allows the cavity length to be adjusted to match the mode-locking frequency. A differential micrometer is used to optimize the cavity length and hence the power output. The entire laser is on a rail composed of three 1-in. (2.54-cm) rods of Invar in order to minimize the cavity-length drift that is due to temperature changes.

The laser is run in a prelasing mode; i.e., the *Q*-switch level is set to permit a low level of cw mode-locked operation between *Q*-switched bursts. This allows the pulse circulating in the cavity to reach a steady-state wave packet before *Q* switching. This is essential for stable shot-to-shot operation. Leakage through one of the cavity mirrors is directed into a fast photodiode. When the *Q*-switched pulse train reaches the appropriate amplitude, the output of the photodiode triggers a single avalanche transistor. This transistor produces a 20-V, 0.5-nsec rise-time pulse. The trigger pulse is split electronically. The first trigger pulse is delayed with an appropriate length of cable in order to select a particular optical pulse in the pulse train. The second trigger pulse has an additional cable delay of several nanoseconds. The two pulses are used to trigger two avalanche transistor chains connected to the Pockels cell. Both sides of the Pockels cell are charged to the quarter-wave voltage, since the optical pulse double passes the cell. The first trigger pulse dumps the charge on one side of the cell and applies the quarter-wave voltage. The pulse polarization is rotated. The other transistor chain is triggered by the second trigger pulse, dumping the charge on the other side of the cell. This returns the *E* field across the cell to zero. The two sides recharge slowly between shots. Fairly successful operation can be achieved with only a single transistor chain and with the other side of the cell tied permanently to high voltage. The crystal, however, undergoes mechanical ringing because of coupling of the electric field to the material's acoustic vibrations through the piezoelectric interaction.[7] This causes the laser prelasing to be unstable. The problem is eliminated by using the second transistor chain to dump the other side of the cell nanoseconds after the pulse has been

switched out but before effective coupling of the E field to the crystal's mechanical degrees of freedom can occur. This procedure also ensures relatively clean optical pulse selection. A main-pulse-to-trailing-pulse ratio of 50:1 is typical with a polarization contrast of several hundred to one.

The pulse, with its polarization rotated, is transmitted through the thin-film dielectric polarizer. Because of the jog in the cavity, the output beam is on a path parallel to the main axis of the cavity. The pulse is picked off by a mirror and directed to a 70-cm lens placed 156 cm away from the curved resonator mirror. The lens focuses the beam into a 5-mm-long potassium trihydrogen phosphate (KTP) frequency-doubling crystal 25 cm away. The resultant 532-nm light is separated from the IR by a dichroic beam splitter. The residual IR light is then directed through a second 5-mm KTP crystal 46 cm away from the 70-cm lens. The green light is separated from the IR again.

The laser performs reliably at a repetition rate of 1 kHz. Typical IR pulse energies are 1 mJ with a maximum of 1.2 mJ. The pulse duration is 100 psec. The output of the first frequency-doubling crystal is typically 650 μJ with a range between 550 and 750 μJ, depending on overall laser alignment. The second crystal produces 50 μJ of frequency-doubled light. The output of the second frequency-doubling crystal is used to pump the first stage of the amplifier, and the output of the first frequency-doubling crystal is used to pump the second and third amplifier stages.

3. DYE LASER SYSTEM

The cw mode-locked Nd:YAG laser is based on a Spectra-Physics Series 3000 laser. This version of the Spectra-Physics laser was modified in two ways. First, a mode locker consisting of a Brewster–Brewster substrate with a 16 mm × 4 mm transducer driven with 1 W of rf power was mounted next to the 10% output coupler. Second, a precision translation stage with a differential micrometer was attached to the original rear mirror mount. The mirror was mounted on the translation stage. This permits differential micrometer control of the cavity length without otherwise modifying the cavity structure. The differential micrometer is essential for achieving adequate cavity-length adjustment. In order to maintain synchronization between the dye pulses and the amplifying pulses, the same rf source is used to drive the mode lockers in both Nd:YAG lasers. Therefore the mode-locking frequency cannot be tuned. The laser produces a stream of 70-psec, Gaussian-shaped, transform-limited pulses spaced 12 nsec apart at average powers of 7.5–8.0 W.

It was found to be necessary to use a high-quality frequency synthesizer (Rhode-Schwartz Model SMX) as the rf source. Lower-quality rf sources exhibit small frequency drifts and phase and frequency modulation. This has a deleterious effect on the laser output, particularly after pulse compression. With a low-quality rf source or with a minute cavity-length mismatch, sudden drops in power of a few percent could be observed on a 1-kHz time scale. These dropouts can be monitored effectively by directing the mode-locked pulse stream into a frequency-doubling crystal and examining the frequency-doubled light on a kilohertz time scale. Although the dropouts are relatively small, they have a dramatic influence on the stability of the pulse-compressed light. It is important to note that if the operation of the laser is monitored only by looking at the pulses on a fast time scale, the dropouts will not be detected. We found the Spectra-Physics cavity construction to be excellent for our laboratory conditions. Small cavity-length adjustments are necessary only after several hours. The overall alignment, which is critical because of the required precise aiming into the pulse compressor, is stable for many months.

The pulse compressor that we used is a Spectra-Physics prototype that was generously donated to us by Spectra-Physics. It is described in detail by Kafka *et al.*[8] The only significant modification to the pulse compressor was to put it into an essentially air-draft-proof Plexiglas box with only small holes to let the laser beam in and out. The box has a small hinged hatch on the side so that we can make adjustments without removing the cover of the box. This was found to be necessary because the compressor is extremely sensitive to normal air currents in the laboratory that are generated by the air conditioning. Without the box, air currents induce pointing instability in the output beam. This makes optimal pumping of a dye laser nearly impossible.

The fiber is single mode and is not polarization preserving. Two independently adjustable quarter-wave plates after the fiber allow the beam polarization to be restored. Over a period of months, the fiber birefringence changes, owing to strain and thermal effects. This is rectified by making small adjustments of the quarter-wave plates. Over the same period, accumulated changes caused by hysteresis in the mirror mounts cause the coupling efficiency into the fiber to decrease by as much as 10%. Fine adjustments of the aiming of the beam into the fiber are sufficient to restore the performance.

An intensity stabilization effect can be achieved in the fiber when the input IR power is adjusted to an optimal value. The result is that the output of the pulse compressor can actually be significantly more stable than the input. As the input power is increased, the output of the compressor follows linearly until it rolls off at higher powers because of stimulated Raman scattering. As the power is increased further, the extent of stimulated Raman scattering becomes so great that the usable output is less than that obtained at lower powers. Thus there is a plateau at which a change in the input power causes a change in the stimulated Raman scattering but does not change the usable output. By adjusting the fiber length and the input power, it is possible to operate the system in the plateau region. This results in stabilization. For powers below the plateau, we have observed that the output fluctuations are correlated with the input fluctuations. At powers above the plateau, the output fluctuations are anticorrelated with the input power; i.e., an increase in the input results in a decrease in the output. Subsequent to our initial observations, this effect recently was modeled theoretically.[9]

With 6 W of input, the pulse compressor puts out 2.5–3.0 W of 3.5-psec, 1.064-μm-wavelength pulses. These pulses sit on a broad pedestal that contains nearly 50% of the energy.[10] There is enough energy in the central portion of the pulse, however, to achieve sufficient second-harmonic average power to pump the dye laser optimally. The nonlinear frequency upconversion suppresses the pedestal, which does not have sufficient intensity to frequency double significantly. The compressed Nd:YAG output is focused into a

5-mm-long KTP crystal by using a 4.5-cm-focal-length lens. The average frequency-doubled power is 750–800 mW, and the pulses are 2.5 psec in duration.

The 532-nm pulse stream is used to pump an astigmatically compensated dye laser.[11] The laser is a standard three-mirror folded cavity. The input mirror, the high reflector, and the fold mirrors have 5-cm radii of curvature. The 15% output coupler is 157 cm (Spectra-Physics), with the output side having the appropriate radius of curvature to recollimate the beam. The output-coupler mirror mount is on a precision translation stage with a differential micrometer to adjust the cavity length. The dye jet is mounted vertically on a rotation stage, which is in turn attached to two translation stages that move up and down and along the Brewster-angle direction of the jet. The translation stages allow us to position the jet for the best optical quality without moving the cavity mirrors or the pump mirror. The rotation stage permits us to adjust the jet angle for optimal performance. This degree of freedom is important. Each of the three mirrors has three micrometer-controlled adjustments. Two of these adjust the mirror angle, and the third sets the distance from the mirror to the jet. The distance adjustments are critical. The optical components are mounted on a three-rod Invar optical rail to minimize cavity-length drift. Wavelength tuning is accomplished with a single-plate birefringent filter.

Dye lasers that are pumped synchronously by long pulses require near-threshold pumping to produce pulse shortening through gain switching of the inversion.[12] Unlike these systems, dye lasers that are pumped synchronously by compressed pulses must be pumped well above threshold to produce subpicosecond pulses. In addition to producing short pulses, the hard pumping results in stable dye laser operation. The pulse shortening appears to be caused by a nonlinear interaction in the dye jet. A study was performed in which the pump spot size in the jet was varied systematically. For each pump spot size, the laser mode volume in the jet was matched to it by maximizing the laser output. The total laser output remained relatively constant for different pump spot sizes (with an appropriate change in the dye concentration). It was found, however, that, as the pump spot size was reduced, the dye pulses became shorter. The optimal situation is that in which the pump spot size is the smallest. This is found easily by observing the transmission of the pump beam through the jet and then maximizing the transmission. This procedure puts the waist of the pump beam in the jet. The positions of the laser cavity mirrors are then adjusted to match the mode volume to this pump spot size.

R6G and DCM dyes were used in the laser. The R6G dye was dissolved in ethylene glycol. The concentration was adjusted to give 95% absorption. This corresponds to the largest usable intracavity gain, thus aiding in short-pulse formation. At higher concentrations, the output power goes down and becomes more unstable. Average powers of as much as 300 mW are obtained for the R6G dye laser, which is tunable over the 560–620-nm wavelength region. The wavelength region of 605–705 nm was covered with DCM dye. With a propylene carbonate–ethylene glycol mixture in a 2:3 ratio used as the solvent, enough dye was dissolved to attain 85% absorption of the green pump. Glycerol was added to stabilize the jet. Average output powers vary over the laser bandwidth from 70 mW at the band edge to 220 mW at the peak of the gain curve.

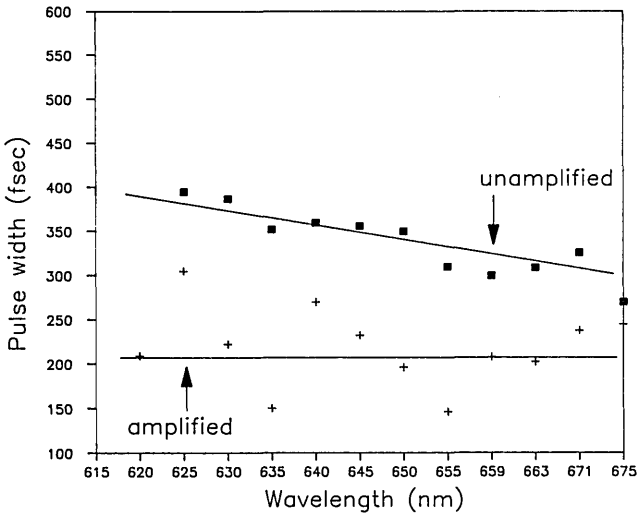

Fig. 2. Dependence of pulse width on wavelength for unamplified (upper trace) and amplified (lower trace) pulses from a DCM dye laser. A hyperbolic-secant-squared pulse shape is assumed. The amplified pulses are shortened by the saturable absorber. To change the wavelength, it is necessary only to tune the birefringent filter and to adjust the cavity length of the dye laser. No other adjustments were made in obtaining these data. This demonstrates the broad-wavelength tunability of the amplified femtosecond dye laser system.

The cavity length at which the shortest pulses are obtained is set by adjusting a differential micrometer and monitoring the pulse width with a real-time autocorrelator. A hard copy of the autocorrelation is obtained for accurate pulse-width determination. Pulses as short as 220 fsec (FWHM), if a hyperbolic-secant-squared pulse shape is assumed (divide the width of the autocorrelation by 1.55), have been obtained. The upper curve in Fig. 2 gives typical unamplified pulse durations measured by autocorrelation for wavelengths covered by DCM. Measurements of the spectral bandwidth of the pulses show that these pulses either are transform limited or within a factor of 1.5 of being transform limited, depending on the model used for the pulse shape. Several recent reports have appeared[1,13,14] of narrower autocorrelation FWHM from this type of laser. In those studies, pellicles, which permit broader bandwidths, were used. All the pulse widths reported in Fig. 2, unamplified and amplified, are for essentially transform-limited pulses and are determined from autocorrelations free from coherence spikes.

4. DYE AMPLIFIER

The dye pulses are amplified with the frequency-doubled output of the *Q*-switched, mode-locked, and cavity-dumped Nd:YAG laser described in Section 2. Amplification with relatively short (70-psec) pump pulses limits the amount of amplified spontaneous emission and results in more-efficient energy transfer between the pump and dye pulses.[15] The amplifier is composed of three stages with a saturable absorber between the second and third stages. All three stages use flowing dye cells (Helma) that are set at Brewster's angle. The first two stages have 1-mm path lengths,

and the last has a 10-mm path length. The stages are pumped longitudinally in an anticollinear configuration that provides good overlap between the dye pulse and the pump pulse. A slightly off-axis geometry is used to avoid the necessity of beam-combining optics. Once the path lengths of the dye and pump pulses between the three amplifier stages have been matched, the overall timing, which is quite critical, is set by shifting the phase of the rf going to the pump laser's mode locker. This is discussed further below.

In all three stages the green pump spot size is made slightly larger than that of the dye beam to avoid inhomogeneous amplification. The 50 μJ green pulse is used to pump the first stage. The dye beam is focused to a spot size of 120 μm (1/e diameter of the E field), using a 25-cm lens. The dye seed pulse energy is 2 nJ. The pump spot is obtained with a 80-cm lens after the second frequency-doubling crystal and a 25-cm lens focusing into the dye cell. The amplification gain in the first stage is a factor of ~250.

The 650-μJ pump pulse from the first frequency-doubling crystal is split into 130- and 520-μJ pulses to pump the second and third stages, respectively. The amplified dye beam is recollimated after the first stage with a 20-cm lens and focused to 360 μm in the second stage, using a 25-cm lens. A gain of ~4 is obtained with a slight increase in the pulse duration. Because of the gain characteristics of the second stage, amplitude fluctuations are reduced.[16] To eliminate both the unamplified pulses and the amplified spontaneous emission, the amplified beam is focused to 35 μm with a 5-cm lens in a saturable absorber (Crystal Violet for R6G wavelengths and Malachite Green for DCM wavelengths). An achromatic doublet lens (Melles Griot) was used to minimize pulse shape distortion from spherical aberration, which can be magnified greatly in the saturable absorber. Absorber concentration was increased until ~70% of the amplified pulse was absorbed. Pulse shortening due to absorption of the pulse leading edge by the saturable absorber yields a net reduction in the pulse duration. The beam is recollimated after the saturable absorber with a 5-cm lens and is directed into the third stage without focusing. The spot size is 1.8 mm. A gain of 15–20 is achieved to produce a net gain of several tens of thousands. The proper pump pulse spot sizes for the second and third stages were obtained by placing a 100-cm lens after the first frequency-doubling crystal and placing a 40-cm lens and a 95-cm lens before the second and the third stages, respectively.

Amplified dye pulse energies of up to 30 μJ were obtained with DCM dye in both the laser jet and the amplifier cells. Energies of as much as 50 μJ were obtained with R6G dye in the laser jet and Rhodamine B in the amplifier cells. With these energies, <300-fsec nearly tranform-limited pulses are obtained routinely. Figure 2 shows the dependence of the pulse duration on the wavelength for the unamplified and amplified pulses for a DCM dye laser. For the sake of comparison, a hyperbolic-secant-squared pulse shape is assumed for both cases. As is shown below, however, an asymmetrical doubled-sided exponential is a more accurate model for the shape of the amplified pulses. The data in Fig. 2 were taken by tuning the birefringent filter and adjusting the cavity length. No other adjustments to the system were made. A pulse-width reduction of up to a factor of 2 occurs after the pulse passes through the amplifier chain.

We have gained quantitative information on the amplified

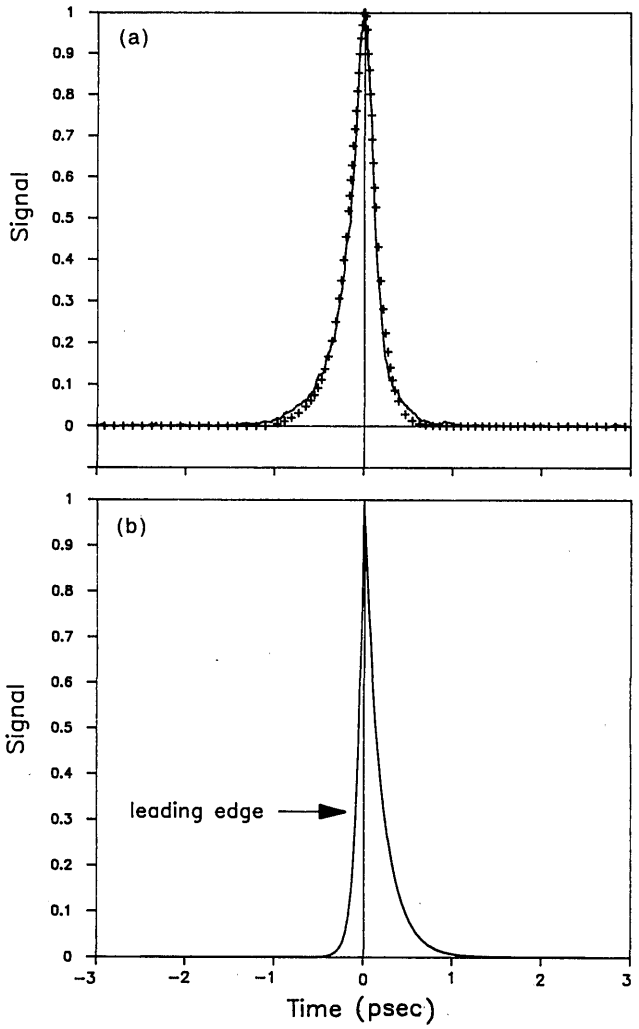

Fig. 3. (a) Instrument response obtained from an electronic-Kerr-effect-induced transient four-wave mixing signal (solid curve). This is a type of three-pulse correlation experiment that, unlike an autocorrelation, is sensitive to asymmetric pulse shapes. The fit (crosses) is obtained with an assumed double-sided exponential pulse shape. (b) The best fit, which has a 70-fsec leading edge and a 200-fsec trailing edge (see the text).

pulse shape by analyzing the signal obtained from a transient-grating electronic-Kerr-effect experiment in the liquid crystal 5CB at a wavelength of 665 nm. The amplified dye pulse is split into three pulses. Two of the pulses are crossed in the sample in time and space to produce an optical interference pattern. The polarizations are chosen to produce only an electronic response.[17] This provides a delta-function system response. The third pulse is delayed and brought into the sample to meet the Bragg diffraction condition of the induced electronic Kerr grating. When the delay line is scanned, a type of three-pulse correlation function is measured. Whereas an autocorrelation always gives a symmetrical curve, the grating experiment yields an asymmetric curve if the pulse is not symmetrical.

Figure 3(a) shows the measured three-pulse correlation function with a calculated curve based on a model of the pulse shape. The calculated curve is obtained by squaring the model function and convolving the squared function with the original function. The model function is a two-

sided exponential. The best fit was obtained with decay constants of 70 and 200 fsec for the leading and trailing edges, respectively. Figure 3(b) displays the actual pulse envelope obtained from the fit. As can be seen, the pulse is quite asymmetrical. This procedure yields valuable information, since it can reveal pulse asymmetry, which gives direct information about the rising and trailing edges of the pulse, either one of which can independently determine the time resolution of a particular experiment.

As the system has been described so far, the amplified pulses can be quite unstable on tens-of-hertz and slower time scales despite stable operation of the dye and pump lasers. The cause of the problem is timing jitter between the pump and dye pulses in the amplifier chain. As mentioned briefly above, the overall timing between the pump pulses and the dye pulse in the amplifier is determined by an electronic phase-shifting device (Merrimac Model PEWM-3-60). The phase shifter produces a variable phase shift of the rf signal fed to the Q-switched laser's mode locker by changing a dc input voltage. Phase shifting the rf signal changes the relative time at which the cavity-dumped pulse leaves the laser. The phase shifter provides a convenient observable index by which to monitor timing fluctuations directly. This is done by delaying the pump pulse with respect to the dye pulse while monitoring the amplified pulses on an oscilloscope. As the pump pulse delay is increased, the amplitude of the amplified pulses decreases until it vanishes when the pulses are no longer overlapped. Once the phase shift is set so that there is no overlap between the pulses, bursts of amplified pulse occur on the oscilloscope trace, providing direct evidence of the timing jitter. The source of the instabilities was investigated by using a different set of phase-shifting electronics and eliminating the phase-shifting electronics completely. In the latter case, the timing was set by adjusting the lengths of the coaxial cables that carry the rf signal. In all cases the optical fluctuations were the same, demonstrating that the source of the fluctuations is not electronic but optical in nature.

We have developed a feedback circuit that varies the rf phase to compensate for the timing jitter in the dye laser. The basic idea is as follows. If the dye pulse comes in before the amplifying pulses, there is zero gain. As the amplifying pulses are phase shifted to earlier time, the dye pulse begins to show gain as it begins to overlap in time with the amplifying pulses. It reaches maximum gain when the phase is set so that the dye pulse arrives just after the amplifying pulses. As the amplifying pulses are shifted to still earlier times, the gain slowly falls because of excited-state relaxation and molecular rotations. If the phase is set somewhat after the peak of the gain, timing jitter will move the dye pulse up and down the gain curve. This produces amplitude fluctuations. The feedback circuit varies the phase to keep the amplified dye pulse constant in amplitude. If there were no other fluctuations, this function would include maintaining the timing so that the dye pulse was always on the same point in the gain curve. The feedback circuit, however, can also compensate for other sources of amplitude fluctuations by shifting the dye pulse position on the gain curve. Since the feedback circuit stabilizes intensity fluctuations from other sources as well as the timing jitter, the timing variations between the amplifying pulses and the dye pulses are still present. Although this should not affect single-pulse pump-probe experiments, it may present a problem for rf-driven experiments probed by the optical pulses.[18]

In the feedback circuit, a photodiode detects a small picked-off piece of the amplified dye pulse. The photodiode is followed by an operational amplifier and a sample-and-hold circuit. The sample-and-hold circuit is triggered at 1 kHz by the clock signal that times the Q-switched laser. There is a one-shot variable delay that is set so that the sample-and-hold circuit detects and holds a voltage proportional to the amplified dye pulse intensity. This voltage is then smoothed by a time constant so that the following circuitry does not attempt to respond to shot-to-shot variations in laser intensity. The output of the smoothed sample-and-hold circuit goes through two operational amplifiers. The first sets the gain of the feedback system. The second determines the set point (average value of the phase shift). The set point is independent of the gain. Finally, there is an operational amplifier clamp circuit to prevent large transients in the optical signal from driving the system past the setting for maximum gain. The slope of the curve changes at the point of maximum gain. Therefore, if the system were allowed to pass this point, the amplification would turn off and would not automatically recover. This clamp is important to prevent the system from turning off if a piece of dust or some other disturbance causes a momentary large reduction in the amplified pulse intensity.

The result of using the feedback circuit is the elimination of the timing jitter and additional stabilization of the long-time-scale (10-msec and longer) intensity fluctuations in the system. It is interesting to note that this type of stabilization and elimination of the timing jitter is not feasible with the standard type of regenerative amplifier. In a regenerative amplifier, a pulse derived from the cw mode-locked laser is injected into a Q-switched cavity. Since there is no mode locker, it is not possible to use the phase-shifting method to eliminate the effects of timing jitter.

5. CONCLUDING REMARKS

The system described above is a versatile source of high-repetition-rate, high-power, subpicosecond transform-limited pulses. The system is tunable over broad wavelength regions. The dye laser can be tuned to any wavelength that a conventional synchronously pumped dye laser system can reach. The wavelength accessibility of the amplifier is similar to that of a conventional flash-lamp-pumped Q-switched (10-nsec pulse) Nd:YAG-laser-based amplifier. The system has proved to be quite reliable. It is run routinely for 12 h a day with a 30-min warm-up period. In one experimental project, the system was run continuously for 60 h. During that time, the Q-switched laser was not touched. The only adjustments made were to the dye laser cavity length every few hours and to the cw mode-locked Nd:YAG laser cavity length less frequently.

It is reasonable to assume that pulses from this type of system could be made shorter in duration. They are currently longer, by a factor of 2 to 4, than amplified pulses from a typical colliding-pulse mode-locked laser. The system described here, however, does not have prism compensation for cavity dispersion in the dye laser, nor does it have a recompression stage after the amplifier. These elements are necessary for obtaining short pulses from an amplified col-

liding-pulse mode-locked laser. Addition of these elements, although straightforward, would greatly reduce the ease of tuning of this system. Now, it is necessary only to tune the birefringent filter and to adjust the cavity length. This makes the system an excellent choice for performing short-time-scale nonlinear laser spectroscopy.

ACKNOWLEDGMENTS

We would like to express our gratitude to the Spectra-Physics Corporation for donating the pulse compressor and other optical elements in this system. We would also like to thank Mark Berg, Department of Chemistry, University of Texas at Austin, for his help on the initial stages of this project and many valuable discussions. This research was supported by the National Science Foundation, Division of Material Research (grant DMR 87-18959). Additional support was provided by the U.S. Office of Naval Research, Physics Division (grant #N00014-85-K-0409). F. W. Deeg would like to thank the scientific committee of the North Atlantic Treaty Organization for a postdoctoral fellowship administered through the German Academic Exchange Service.

REFERENCES

1. A. M. Johnson, and W. M. Simpson, J. Opt. Soc. Am. B **2,** 619 (1985).
2. J. D. Kafka and T. Baer, in *Ultrashort Pulse Spectroscopy and Applications,* M. J. Soileau, ed., Proc. Soc. Photo-Opt. Instrum. Eng. **533,** 38 (1985).
3. J. P. Ryan, L. S. Goldberg, and D. J. Bradley, Opt. Commun. **27,** 127 (1978); B. Couillaud, V. Fossati-Bellani, and F. Mitchell, in *Ultrashort Pulse Spectroscopy and Applications,* M. J. Soileau, ed., Proc. Soc. Photo-Opt. Instrum. Eng. **533,** 46 (1985).
4. R. L. Fork, B. I. Greene, and C. V. Shank, Appl. Phys. Lett. **38,** 671 (1981).
5. G. T. Harvey, C. W. Gabel, and G. Mourou, Opt. Commun. **36,** 213 (1981).
6. R. J. D. Miller, L. Min, and M. A. Shragowitz, Opt Commun. **62,** 185 (1987); T. Sizer II and I. N. Duling III, IEEE J. Quantum Electron. **QE-24,** 404 (1988).
7. R. P. Hilberg and W. R. Hook, Appl. Opt. **9,** 1939 (1970); W. D. Fountain, Appl. Opt. **10,** 972 (1971).
8. J. D. Kafka, B. H. Kolner, T. Baer, and D. M. Bloom, Opt. Lett. **9,** 505 (1984).
9. J. D. Kafka and T. M. Baer, IEEE J. Quantum Electron. **QE-24,** 341 (1988); M. Kuckartz, R. Schultz, and H. Harde, J. Opt. Soc. Am. B **5,** 1353 (1988).
10. D. Grischkowsky and A. C. Balant, Appl. Phys. Lett **41,** 1 (1982).
11. H. W. Kogelnik, E. P. Ippen, A. Dienes, and C. V. Shank, IEEE J. Quantum Electron. **QE-8,** 373 (1972).
12. J. Kluge, D. Wiechert, and D. von der Linde, Opt. Commun. **45,** 278 (1983).
13. A. M. Johnson and W. M. Simpson, IEEE J. Quantum Electron. **QE-22,** 133 (1986).
14. R. Iscoff, Lasers Optron. **7,** 47 (1988).
15. T. Sizer II, J. D. Kafka, I. N. Duling III, C. W. Gabel, and G. A. Mourou, IEEE J. Quantum Electron. **QE-19,** 506 (1983).
16. T. L. Koch, L. C. Chiu, and A. Yariv, J. Appl. Phys. **53,** 6047 (1982).
17. J. Etchepare, G. Grillon, J. P. Chambaret, G. Hamoniaux, and A. Orszag, Opt. Commun. **63,** 329 (1987).
18. K. J. Weingarten, M. J. W. Rodwell, and D. M. Bloom, IEEE J. Quantum Electron. **QE-24** 198 (1988), and references therein.